

## A RADIAL VELOCITY SEARCH FOR $p$ -MODE PULSATIONS IN $\eta$ BOOTIS

TIMOTHY M. BROWN AND EDWARD J. KENNELLY

High Altitude Observatory/National Center for Atmospheric Research,<sup>1</sup> P.O. Box 3000, Boulder, CO 80307;  
brown@hao.ucar.edu, kennelly@hao.ucar.edu

SYLVAIN G. KORZENNIK, PETER NISENSEN, AND ROBERT W. NOYES

Harvard-Smithsonian Center for Astrophysics, 60 Garden Street, Cambridge, MA 02138;  
sylvain@cfasp30.harvard.edu, nisenso@cfasp30.harvard.edu,  
noyes@cfasp30.harvard.edu

AND

SCOTT D. HORNER

Astronomy & Astrophysics, Pennsylvania State University, 525 Davey Laboratory,  
University Park, PA 16802-6305; horner@astro.psu.edu

Received 1996 March 21; accepted 1996 August 5

### ABSTRACT

The subgiant  $\eta$  Boo (G5 IV) has been reported to show  $p$ -mode pulsations, as evidenced by variations in the equivalent width of its hydrogen Balmer lines (reported by Kjeldsen et al.). In an attempt to confirm this report, we observed  $\eta$  Boo's radial velocity with the AFOE spectrograph for a total of 22 hours spread over seven successive nights in 1995 March. We find no evidence for the presence of excess power at the frequencies reported by Kjeldsen et al.; our upper limit corresponds to typical mode amplitudes of  $0.5 \text{ m s}^{-1}$ , about 3 times smaller than the velocity amplitudes they inferred. Signals with amplitudes larger than  $0.5 \text{ m s}^{-1}$  may be present at other frequencies within the 0–1000  $\mu\text{Hz}$  range, but evidence for such signals is scanty, and typical mode amplitudes greater than  $1.5 \text{ m s}^{-1}$  are clearly inconsistent with our observations.

*Subject headings:* stars: individual ( $\eta$  Bootis) — stars: oscillations — techniques: radial velocities

### 1. INTRODUCTION

Knowledge of the pulsation frequencies of Sun-like stars would help answer many questions connected with the structure and evolution of stars. For this reason, the last decade has seen many efforts to solve the challenging problem of detecting and characterizing pulsations with very small amplitudes. To date, however, these efforts have not been successful, and there remains no unambiguous observation of  $p$ -modes on another Sun-like star. Recently, Kjeldsen et al. (1995, hereafter KBVF) have described a promising approach to this problem, namely, measurement of the equivalent width of a number of hydrogen Balmer lines as a proxy for the small temperature changes associated with low-amplitude stellar pulsation. In the first application of this method, these authors searched for evidence of  $p$ -modes in the nearby star  $\eta$  Boo (G5 IV). Subgiants like  $\eta$  Boo are attractive candidates for such studies because theory predicts relatively large surface amplitudes for solar-like pulsations in these stars ( $\delta I/I = 2\text{--}3 \times 10^{-5}$ , or  $\delta v = 1\text{--}2 \text{ m s}^{-1}$ ). On the other hand, the low mean density of subgiants implies a small frequency separation between different oscillation modes of the star, which causes difficulties in the interpretation of the interrupted data that can be obtained from single low-latitude telescopes. (For details of these and other expected properties of pulsations in Sun-like stars, see Brown & Gilliland 1994.)

KBVF observed  $\eta$  Boo for six nights from the 2.5 m Nordic Optical Telescope on La Palma and reported a successful detection of 13 oscillation modes, all in the frequency band between 700 and 1000  $\mu\text{Hz}$ . KBVF identified the modes as having angular degree  $l$  in the range 0–2, and typical relative equivalent width amplitudes  $\delta W/W$  of

about  $4.5 \times 10^{-5}$ , or 45 parts per million (ppm). Based on simple theoretical considerations, they estimated a typical velocity amplitude of  $1.6 \text{ m s}^{-1}$ . The largest amplitude mode seen had a frequency of 853.7  $\mu\text{Hz}$  and  $\delta W/W = 75$  ppm, corresponding to a velocity amplitude of about  $2.7 \text{ m s}^{-1}$ . The mode frequencies identified by KBVF were characterized by a large frequency separation (the difference in frequency between two modes with  $l = 0$  and consecutive values of the radial order  $n$ ) equal to 40.3  $\mu\text{Hz}$ ; the characteristic frequency spacing between adjacent peaks in the power spectrum is half of this value, or 20.15  $\mu\text{Hz}$ . These values are consistent with model calculations of pulsation frequencies in stars like  $\eta$  Boo; the frequencies themselves have been used in several detailed comparisons with the results from grids of stellar models aimed at refining estimates of  $\eta$  Boo's structural parameters and evolutionary state (Christensen-Dalsgaard, Bedding, & Kjeldsen 1995; Guenther & Demarque 1996).

In view of the importance of these developments, we decided to attempt to confirm the pulsation characteristics of  $\eta$  Boo, using precise Doppler-shift measurements. As we shall describe below, this attempt was unsuccessful; indeed, it yielded a significant nondetection of the frequencies reported by KBVF at amplitudes several times smaller than those inferred from their observations.

### 2. OBSERVATIONS AND DATA REDUCTION

We observed  $\eta$  Boo for seven nights (1995 March 14 to March 20) using the Advanced Fiber Optic Echelle (AFOE) on the 1.5 m Tillinghast telescope located at the Whipple Observatory at Mount Hopkins, AZ. The AFOE is a fiber-fed cross-dispersed echelle spectrograph that is optimized for precise and stable Doppler measurements, as described by Brown et al. (1994). As configured for these observations, it covered 160 nm of spectrum lying between 393 and 665

<sup>1</sup> The National Center for Atmospheric Research is Sponsored by the National Science Foundation.

nm at resolution  $R \equiv \lambda/\delta\lambda$  of roughly 32,000. The wavelength reference used for these observations was a ThAr emission-line spectrum brought into the spectrograph on a second optical fiber immediately adjacent to that carrying the starlight. We employed a comparatively low spectral resolution in order to minimize aliasing of the narrow ThAr lines and accompanying Doppler instability. We did not attempt to duplicate KBVF's measurements of Balmer line equivalent widths because the photon noise imposed by the relatively small bandwidth in these lines results in a detection limit significantly higher than the expected signal.

All spectra of  $\eta$  Boo had exposure times of 120 s; with CCD readout and other overhead, the interval between successive spectra averaged 146 s. In all, 555 spectra were obtained; spotty clear weather resulted in a duty cycle of only 15% for the 6.2 day interval spanned by the observations.

Reduction of the CCD images to one-dimensional spectra proceeded via the usual steps of bias subtraction, integration of the signal across orders of the echelle spectrum, correction for scattered light, and flat-fielding using spectra of a quartz-halogen lamp. A few aspects of this process require further comment. First, we estimated the detected signal at each point along the dispersion as a simple sum of the bias-corrected pixel intensities over a window of suitable width centered on the order. This procedure is justified by the relative unimportance of read noise compared to photon shot noise in the spectra. Second, the scattered light correction depends on a simple model of the spatial distribution of scattered light on the detector. This model has proved to be inadequate in some respects, so that small errors that vary smoothly with wavelength are introduced into the one-dimensional spectra. We shall return to this problem below. Finally, flat-fielding is performed on the one-dimensional spectra rather than on the two-dimensional CCD images. This procedure is formally incorrect but in practice yields better results than two-dimensional flat-fielding because it avoids division by poorly determined gain values at the edges of the spectrum orders.

After reduction to one-dimensional spectra, the observations were analyzed to yield (among other parameters) shifts (in pixel units) of the stellar spectrum relative to a standard spectrum obtained near the center of the run, and shifts of the ThAr spectrum relative to a similar standard. The process used to compute these shifts is complicated and will be described in detail elsewhere. Its essential features are as follows: For each observation, we fit models to both the stellar and the ThAr spectra by  $\chi^2$  minimization. A noise model, which takes account of both photon shot noise and read noise, allows quantitative estimates of the formal errors in the fitted parameters. For the ThAr model, parameters that are fitted include displacement and distortion coefficients describing the positions of the observed ThAr lines relative to those in the standard spectrum, the intensity of each ThAr line, and parameters in a physically motivated model of the spectrograph point-spread function (PSF). A byproduct of the ThAr fit is an accurate dispersion curve, i.e., a parameterization of the curve relating vacuum wavelength to pixel position on the CCD. The basis of the stellar spectrum model is an observed spectrum of the target star from which the spectrograph point-spread function has been removed by deconvolution. In fitting the model, this spectrum is convolved with the PSF determined from the ThAr spectrum fitting, and then displaced and distorted to

yield the best fit to the observed spectrum. Parameters that emerge from the fit are the coefficient describing the spectrum displacement and distortion and parameterizations of the continuum and residual background light functions. The fitting process proceeds independently for each of the 23 spectrum orders. We difference the stellar and ThAr displacements for each order and multiply by an appropriate factor (determined from the dispersion functions) to yield a velocity in units of  $\text{m s}^{-1}$ . Finally, we form a weighted mean of the velocities for all the 23 spectrum orders, with weights inversely proportional to the time series variance of the velocity for each order. The resulting velocity estimate is interpreted properly as the star's velocity measured in the laboratory frame, with an arbitrary zero point that is determined jointly by the stellar velocity at the time of the stellar standard spectrum and by the spectrograph's dispersion function at the time of the ThAr standard.

After correcting for telescope motion relative to the solar system barycenter and subtracting a constant value, the resulting velocities are as plotted in Figure 1. Eta Boo is a spectroscopic binary with a well-determined orbit and a period of approximately 495 days (Bertiau 1957). The dashed line in Figure 1 is Bertiau's ephemeris velocity, translated in time by  $-10$  days; the dot-dashed line shows the effect of adopting the orbital ephemeris without change. To shift the ephemeris curve by 10 days requires adjusting the orbital period by  $-0.22$  days, or the epoch by  $-10$  days, or some combination of the two. Since the quoted probable (not standard) errors on the period and the epoch are 0.05 and 2.4 days, respectively, an adjustment of the required magnitude is not implausible. Further measurements over a larger part of the orbit will be necessary to determine whether such an adjustment is in fact appropriate. For the current purposes, however, it is sufficient to note that the rotational and orbital motions of the Earth, which cause a velocity variation of more than  $3 \text{ km s}^{-1}$  over the 7 day observing interval, are accounted for correctly with an error of at most  $30 \text{ m s}^{-1}$ . The accuracy of the velocity calibration is important because we desire to compare our measured mode amplitudes (or upper limits) to those inferred by KBVF. Based on the accuracy with which orbital motions are measured, we conclude that the

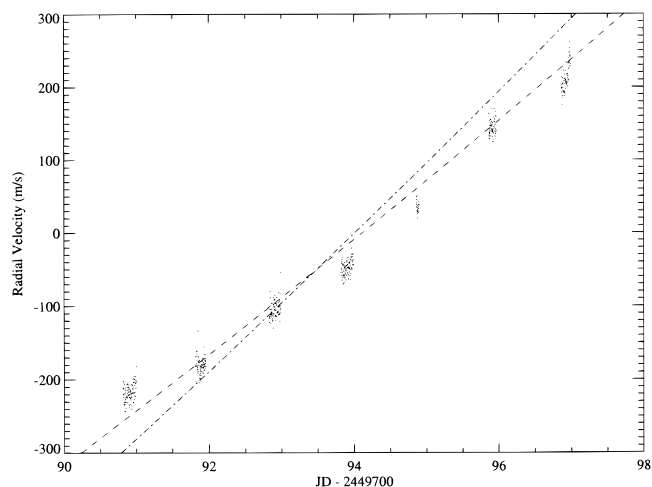


FIG. 1.—Barycentric velocity of  $\eta$  Boo shown for the full seven nights of observations. The dot-dashed line is Bertiau's ephemeris for the orbital motion of  $\eta$  Boo (shown with an arbitrary zero point). The dashed line is the same ephemeris shifted in time by 10 days, with a different zero point. Five spurious data points have been removed from the data for JD 2449790, as described in the text.

velocity scaling that we use is in error by less than 1%, and possibly much less.

Although the stability of the velocity measurements on timescales of hours to days is good, there remain residual drifts in the velocity zero point from night to night and during each night. The known instrumental drifts are of about the same size as the apparently regular derivations of the velocity from the ephemeris values, seen in Figure 1. Therefore, we do not consider these variations to be significant in themselves. These drifts do, however, contribute apparent velocity discontinuities at the beginning and end of each night in the time series. These discontinuities spread spurious power into all frequencies in the spectrum, and thus they are detrimental to a search for pulsations even when the frequencies of interest are greater than 500  $\mu\text{Hz}$ . Also, some improvement in the time series rms may be obtained by choosing the weights for averaging velocity over orders on a nightly basis, rather than using the same set of weights for the entire run. Therefore, we weighted the data in this fashion, and in addition we fitted and subtracted from each night's raw velocity time series a linear function of time. The resulting time series shows one large ( $200 \text{ m s}^{-1}$ ) short-lived (five consecutive images) excursion, which coincides with a dip in the detected intensity to about 10% of its typical value. We discarded these five points, after which the time series displayed an rms variation of  $10.3 \text{ m s}^{-1}$ . These five data points have been excluded from the data plotted in Figure 1.

Finally, we investigated the detrended velocity time series for correlation with similarly detrended series of other parameters emerging from the  $\chi^2$  fitting process. We found the velocity to be correlated significantly with the mean intensity of the spectrum (i.e., the total amount of light coming into the spectrograph). We believe that this correlation is related to the incorrect background subtraction described above; the effect is thus amenable to treatment using improved reduction methods. But since the magnitude of the effect was rather small and the amount of work involved in reprocessing was very large, we chose instead to subtract from the velocity time series a constant factor times the intensity series, with the factor chosen so that the result was uncorrelated with intensity. This decorrelation process reduced the rms to  $9.5 \text{ m s}^{-1}$ . It was this detrended and decorrelated velocity time series that we used in all the subsequent analysis.

The formal error of the spectrum shift parameter produced by the  $\chi^2$  fit averages  $8.5 \text{ m s}^{-1}$ . This number is in fairly good agreement with the observed velocity time series rms, which suggests that the observed velocity variations are dominated by known noise processes, namely, photon shot noise and CCD readout noise. The difference between the two values does, however, leave room for a signal of stellar origin and of substantial size (up to about  $4 \text{ m s}^{-1}$  rms, or more if the photon noise is overestimated).

The estimated spectrum shift just described corresponds to a strength-weighted average over all the lines in the observed part of the stellar spectrum. It is worth noting that, for stellar  $p$ -modes, one expects the Doppler signals for all spectrum lines to be in phase, regardless of their depth of formation. The solar spectrum is indeed observed to behave this way in response to the Sun's  $p$ -modes (Ronan, Harvey, & Duvall 1991). The reason is related to the physics of the modes: for a  $p$ -mode to attain a significant amplitude, the upper boundary of the cavity in which the mode is confined

must lie below the region in which damping mechanisms are important, i.e., below the stellar photosphere. Thus, the largest amplitude  $p$ -modes should be evanescent in and above the photosphere, with large (nominally infinite) vertical phase speeds. This implies that the Doppler shifts from all lines are in phase, and one may average them as we do without loss of sensitivity.

### 3. TIME SERIES ANALYSIS

We computed the power spectrum of the velocity series using Scargle's (1982) algorithm for unevenly spaced data. Figure 2 shows the entire spectrum out to 3000  $\mu\text{Hz}$  (slightly below the Nyquist frequency for our sampling rate). The evident comblike structure that appears throughout the spectrum results from the gapped window function. As the spectrum is displayed, a pure sinusoid with amplitude  $a \text{ m s}^{-1}$  would appear as a cluster of peaks, the largest of which would have power equal to  $a^2$ . There is a small amount of excess power at frequencies below 1000  $\mu\text{Hz}$ , and a sharp cutoff below 50  $\mu\text{Hz}$ , at which the linear detrending attenuates the very lowest frequencies. Otherwise the power distribution is fairly flat, consistent with broadband noise. The mean power level corresponds to an amplitude of  $0.9 \text{ m s}^{-1}$ , and the largest peak in the spectrum, at 754  $\mu\text{Hz}$ , corresponds to a sinusoid with an amplitude of  $2.6 \text{ m s}^{-1}$ .

The top panel of Figure 3 shows power in the frequency range from 700 to 1000  $\mu\text{Hz}$ , with the frequencies reported by KBVF indicated with vertical dashed lines. There are evidently very few coincidences between KBVF's frequencies and peaks in our velocity power spectrum. The bottom panel of Figure 3 shows a CLEANed spectrum (see, e.g., Roberts, Lehar, & Drehar 1987) with the KBVF frequencies overlain. As with the raw power spectrum, there is poor agreement between the peaks in the spectrum and the KBVF frequencies.

It is immediately apparent from Figure 3 that our observations do not support KBVF's conclusions, but to what extent are the two sets of observations in conflict? To answer this question we consider two narrower questions, one very specific and one less so. First we suppose that

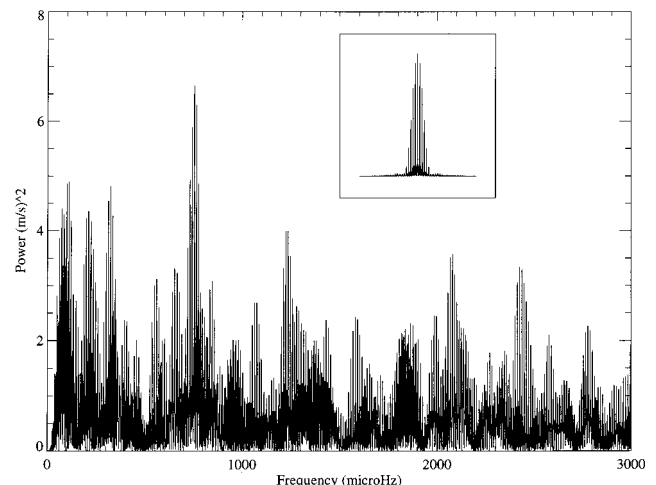


FIG. 2.—Observed power spectrum of  $\eta$  Boo. Power units are such that a pure sinusoid with semi-amplitude  $1 \text{ m s}^{-1}$  would yield a cluster of peaks (because of the gapped window function) whose highest peak would show power = 1. This spectrum shows the entire range of frequencies sampled by the AFOE data. The inset shows the power spectrum of the window function for our observations, illustrated at the same scale as the main figure, for a signal amplitude of  $1.5 \text{ m s}^{-1}$ .

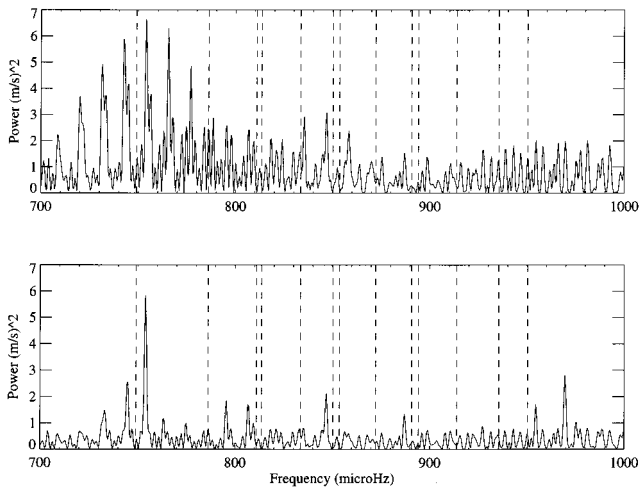


FIG. 3.—*Top*: The power spectrum of Fig. 2, but replotted to show only the range 700–1000  $\mu\text{Hz}$ , and with the frequencies identified as  $p$ -modes by KBVF indicated with vertical dashed lines. *Bottom*: The same spectrum, with KBVF's frequencies, after application of a CLEAN algorithm in an attempt to remove the effects of the window function.

$\eta$  Boo does in fact pulsate with the frequencies reported by KBVF, and that the statistical distribution of amplitude for each mode is of the same form as that found for the Sun. However, we take the characteristic mode amplitude (estimated as  $1.6 \text{ m s}^{-1}$  by KBVF) to be a free parameter, and we ask how large this characteristic amplitude may be without conflicting seriously with our observed spectrum. Because this hypothesis is so specific, it is possible to test it in a sharp and satisfactory way. Second, we ask whether the velocity data provide evidence for any pulsations in  $\eta$  Boo, even if not at the frequencies reported by KBVF. This question allows much more room for supposition, so the answer is not as clear as one would like.

### 3.1. Limits on the Amplitudes of Specified Frequencies

Our approach to testing the hypotheses described above was first to compute from the observed power spectrum a small number of statistics that are related in a plausible way to the presence of a set of modes with specified frequencies. Then, using a statistical model of the pulsation and noise processes, with the characteristic mode amplitude as an adjustable parameter, we created many realizations of velocity time series sampled on the same time grid as our observations. We computed the power spectra of these artificial time series, and from each spectrum we generated the same statistics that were computed from the observations. By comparing each observed statistic with the distribution of corresponding values from the artificial time series, we estimated a probability that the observed time series was consistent with the amplitude assumed when generating the artificial time series.

We modeled the time series as the sum of Gaussian-distributed uncorrelated noise and 13 sinusoids with the frequencies given by KBVF. We chose the noise amplitude to give the correct power density averaged over the two bandpasses [0–500  $\mu\text{Hz}$ ] and [1000–1500  $\mu\text{Hz}$ ]. Because the noise was uncorrelated between samples, the expectation value of its power spectrum is independent of frequency. In this respect, the model does not reflect accurately the observed spectrum, in which the power increases somewhat at frequencies below 1000  $\mu\text{Hz}$ . The average power in the [500–1000  $\mu\text{Hz}$ ] band was very nearly correct, however,

and the uncertainties associated with the observed power spectrum are large enough that a more complex model seemed unwarranted. We took the expectation values of the mode amplitudes to depend on the angular degree  $l$  (as identified by KBVF), but not on frequency. Denoting the characteristic mode amplitude by  $A_m$ , the mode expectation values  $\langle A_l \rangle$  were given by

$$\langle A_l \rangle = \begin{cases} 1.1A_m & (l = 0, 1); \\ 0.55A_m & (l = 2). \end{cases} \quad (1)$$

We chose the scaling constants 1.1 and 0.55 so that the mode amplitudes for  $l = 2$  were half as large as for  $l = 0, 1$ , and the power averaged over KBVF's identified modes was unity. With this normalization and the mode identifications given by KBVF (three of the 13 modes are identified as  $l = 2$ ), the average power per mode equals  $A_m^2$ . Modes with  $l = 2$  were assigned low amplitudes because averaging over the visible hemisphere of a star suppresses the net oscillating signal for these modes. The chosen suppression factor of 0.5 is only approximate, but uncertainties in the center-to-limb dependence of the Doppler signal make it difficult to justify a more sophisticated estimate. Similarly, we did not impose a frequency dependence because there is little justification, either in theory or in KBVF's power spectrum, for choosing one form of frequency variation over another. Mode amplitudes were chosen from an exponential distribution in power, i.e.,

$$P(A_l^2) = \frac{1}{\langle A_l^2 \rangle} \exp\left(\frac{-A_l^2}{\langle A_l^2 \rangle}\right), \quad (2)$$

where  $P(A_l^2)$  is the probability density for the power in a given mode. This distribution is the same as that observed for  $p$ -modes in the Sun. An implication of this distribution is that the observed power in a single mode or even in the sum of several modes can be surprisingly variable. This variability is thought to be intrinsic to the driving and damping processes that determine the amplitudes of solar-like oscillations, so it is important to represent it correctly in the model time series. For each realization, the amplitudes of the 13 sinusoids were chosen independently of one another, and the phases were also independent and distributed uniformly between 0 and  $2\pi$ .

The simplest statistic related directly to the presence of the 13 modes is  $P_{13}$ , which we defined as the power averaged over 13 narrow bandpasses centered on the reported mode frequencies. Since the frequency uncertainties quoted by KBVF range from 0.2 to 1  $\mu\text{Hz}$ , we used bandpass widths of 4  $\mu\text{Hz}$ , i.e.,  $\pm 2\sigma$  for the least certain measurements. For the observed (not CLEANed) velocity power spectrum,  $P_{13}$  is about 25% smaller than the average power in the [500–1000  $\mu\text{Hz}$ ] band, and about 15% smaller than that averaged over the combined [0–500  $\mu\text{Hz}$ ] and [1000–1500  $\mu\text{Hz}$ ] bands. To estimate the probability distribution for  $P_{13}$  as a function of  $A_m$ , we generated 1000 artificial time series for a range of characteristic amplitude values  $A_m$ . For the 1000 artificial time series corresponding to each of the characteristic amplitudes  $A_m = 0., 0.4, 0.5, 1.0, 1.6 \text{ m s}^{-1}$ , the number  $n$  of realizations displaying values of  $P_{13}$  as small or smaller than that observed were  $n = 313, 63, 38, 7$ , and 0, respectively. We conclude that our observations are consistent with the absence of any excess power at KBVF's frequencies; specifically, characteristic mode amplitudes of  $1.6 \text{ m s}^{-1}$  are inconsistent with our observations with

99.9% confidence, and amplitudes of  $0.5 \text{ m s}^{-1}$  are inconsistent with 95% confidence. Therefore, we are unable to confirm the presence of the frequencies reported by KBVF, and in fact we can set upper limits on possible mode amplitudes at the specified frequencies that are significantly smaller than those which they estimated.

### 3.2. Search for Modes with Other Frequencies

Although the frequencies found by KBVF are not present in our data, there may be evidence for pulsations at other frequencies. Since the frequencies of such hypothetical oscillation modes are not known a priori, it is necessary to search the spectrum for evidence of excess power showing frequency regularities that might reveal the presence of  $p$ -modes. Because of the large number of such possible regularities, the likelihood of a false detection is increased, and the limits one can place on signal amplitudes are correspondingly poorer.

Two features of the observed power spectrum suggest the presence of  $p$ -modes. First, there is a slight excess of total power in the  $[500\text{--}1000 \text{ }\mu\text{Hz}]$  band, relative to the average of the two neighboring bands. The total power in the three bands  $[0\text{--}500]$ ,  $[500\text{--}1000]$ , and  $[1000\text{--}1500] \text{ }\mu\text{Hz}$  is in the ratio of  $(1.04:1.00:0.79)$ . The power density evidently drops somewhere near  $1000 \text{ }\mu\text{Hz}$ , a behavior that is consistent with expected  $p$ -mode properties for  $\eta$  Boo. Second, the peak at  $754 \text{ }\mu\text{Hz}$  is substantially larger than any other feature in the spectrum; perhaps it is itself a  $p$ -mode.

To address these issues we proceeded as before, comparing observed properties of the power spectrum with similar ones computed from 1000 realizations of artificial time series. As before, each artificial time series included signals from a set of  $p$ -modes with KBVF's frequencies and with specified characteristic mode amplitudes. The only difference was that the power spectrum statistics computed were not specific to the mode frequencies, but rather they would give similar values for any similar distribution of mode frequencies.

The most useful statistics that we computed for this purpose were the mean and the maximum power within the  $[500\text{--}1000 \text{ }\mu\text{Hz}]$  band. We found that the excess mean power within this band is not significant; excess power as large or larger than that observed occurred in 27% of the artificial time series for which the characteristic mode amplitudes were zero. On the other hand, imposing characteristic mode amplitudes of  $1.6 \text{ m s}^{-1}$  resulted in the mean power being larger than that observed in 95% of the cases. Thus, if  $p$ -modes exist on  $\eta$  Boo with a frequency distribution that is at all similar to that of KBVF, it is unlikely that their characteristic amplitudes exceed  $1.6 \text{ m s}^{-1}$ . The amplitude at which the simulated power exceeded the observed power in about half the cases was roughly  $0.3 \text{ m s}^{-1}$ . The large peak at  $754 \text{ }\mu\text{Hz}$  proves to be either insignificant or anomalous, depending upon one's assumptions. In simulations in which the characteristic mode amplitude was set to zero, a peak as large as the observed one appeared in the  $[500\text{--}1000 \text{ }\mu\text{Hz}]$  band in only 3.8% of the cases. Thus, if our search is confined to the  $[500\text{--}1000 \text{ }\mu\text{Hz}]$  region on a priori grounds based on the expected acoustic cutoff frequency  $\omega_{ac}$ , the  $754 \text{ }\mu\text{Hz}$  peak appears to be marginally significant. But the likelihood of finding a peak of this size somewhere within the spectrum (which is meaningfully sampled out to about  $3000 \text{ }\mu\text{Hz}$ ) is 6 times larger, or about 20%. Therefore, we view the presence of this peak within the frequency band

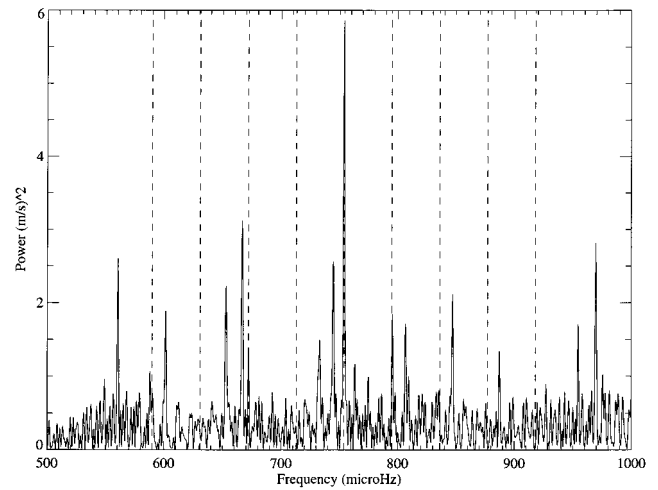


FIG. 4.—The CLEANed power spectrum of Fig. 3, with superposed lines indicating the frequencies that contribute to the largest comb response output located within this frequency range. Aside from the central peak, the peaks that contribute to this (relatively large) value of the comb response are not the largest ones in this part of the spectrum.

in which pulsations are expected as suggestive but inconclusive evidence for  $p$ -modes.

Finally, we have computed the “comb response” defined by KBVF. The comb response is a generalization of the power spectrum of the power spectrum, involving the product of measured power values at several equally spaced distances in frequency from a specified point. Unsurprisingly, the largest values of the comb response for the AFOE data were obtained when the comb was centered at  $754 \text{ }\mu\text{Hz}$ , the frequency of the largest peak. The frequency splitting at which the maximum occurs is  $41.0 \text{ }\mu\text{Hz}$ , a splitting that is similar to (but distinguishable from) the  $40.3 \text{ }\mu\text{Hz}$  splitting derived by KBVF. The maximum numerical value obtained for the comb response for the observed time series is not, however, unusually large compared to maximum values found in the simulated time series with mode amplitudes set to zero; equal or larger values were found in 25% of the artificial cases, if the comb was centered on the largest peak in the  $[500\text{--}1000 \text{ }\mu\text{Hz}]$  band. Moreover, an examination of the frequencies in a CLEANed power spectrum corresponding to those that contribute to the maximum comb response discourages the belief that a clear picket-fence structure has been found (see Fig. 4). Centering the comb on each of the nine largest peaks [those with power greater than  $2.5 (\text{m s}^{-1})^2$ ] between  $700$  and  $1000 \text{ }\mu\text{Hz}$  in the CLEANed spectrum yields similarly inconclusive results. Peaks are found in the comb response in each case, but in no case are the peak amplitudes compellingly large, nor is there an obvious tendency for similar frequency splittings to recur among the various center positions. In one case (that centered at  $652.5 \text{ }\mu\text{Hz}$ ), a peak in the comb response occurs at a splitting of  $40.2 \text{ }\mu\text{Hz}$ , close to the value reported by KBVF. This peak is, however, the smallest of five moderate-sized peaks that occur at various splittings for the given center position, and we believe that the coincidence with the KBVF splitting is fortuitous.

## 4. DISCUSSION

In the previous section we showed that the frequencies identified by KBVF are not present in our velocity time series, with an amplitude upper limit of approximately  $0.5 \text{ m s}^{-1}$ . This limit is about  $\frac{1}{3}$  of the velocity amplitude

inferred by KBVF from their observations of Balmer line equivalent widths. Pulsations with other frequencies may be present in our time series with amplitudes as large as about  $1 \text{ m s}^{-1}$ , but there is no evidence for any single mode with amplitude greater than  $2.5 \text{ m s}^{-1}$ , and if one assumes that roughly one dozen modes should be excited to similar amplitudes, then the maximum allowable amplitude is about  $1.5 \text{ m s}^{-1}$ .

There appear to be three possible explanations for these differences between our observations and those of KBVF.

1. Either or both sets of observations may be in error, as a result of noise or some other process leading to apparently reasonable conclusions that are in fact incorrect. It is hard to dismiss this possibility. Both experiments were done carefully, but the sources of error in measurements of this precision are often subtle and difficult to identify. The relatively small duty cycle of the current observations is particularly worrisome in this regard, though we have been unable to devise a mechanism whereby the duty cycle would necessarily lead to the results we have obtained.

2. The connection between Doppler shift and the Balmer line equivalent widths may be calibrated incorrectly. The sense of the error would need to be that a given Doppler shift yields a significantly larger variation in Balmer line equivalent width than that calculated by KBVF. Observations of the solar  $p$ -modes (Ronan et al. 1991) suggest exactly the opposite, namely, that the Balmer lines tend to remain constant with  $p$ -mode phase, while most photospheric lines show measurable equivalent width variations. More observational work (both on the Sun and on larger amplitude pulsators such as  $\delta$  Scuti stars) is needed to resolve this question.

3. The frequencies or amplitudes of  $p$ -modes in  $\eta$  Boo may have changed in the year that elapsed between the two

sets of observations. A uniform frequency shift of a few  $\mu\text{Hz}$  would suffice to spoil the expected detection of power at KBVF's frequencies. Conversely, a shift of a few  $\mu\text{Hz}$  between KBVF's spectrum and ours could substantially improve the agreement. For instance, shifting our CLEANed power spectrum (Fig. 3, bottom panel) to higher frequencies by about  $4 \mu\text{Hz}$  would cause coincidences between four of our lesser peaks and their peaks at 749.1, 811.0, 850.3, and 890.8  $\mu\text{Hz}$ . The low-degree solar  $p$ -modes are known to change frequency with changing levels of magnetic activity (e.g., Régulo et al. 1994). In the solar case, however, the observed relative frequency changes are typically less than one part in  $10^4$ . The necessary relative frequency shifts in  $\eta$  Boo would be about 50 times larger, a magnitude of variation that seems unlikely. Statistical changes in mode excitation should have been accounted for properly in our time series modeling. More systematic changes in mode amplitudes (due, for example, to changes in the  $p$ -mode driving or damping) seem unlikely but are hard to rule out because of our present limited understanding of the processes that drive and damp solar-like  $p$ -modes.

Further observations of  $\eta$  Boo are necessary, both with equivalent width methods to verify KBVF's results directly, and with Doppler measurements to reduce the Doppler detection limit still further. We believe that significant improvements in the detectable signal can be made with existing equipment, so we intend to continue study of this interesting star.

We are grateful for useful conversations with H. Kjeldsen, S. Frandsen, and M. Viskum, and for the assistance we have received from B. Van't Sant, T. Groner, and the other staff members at the Whipple Observatory.

#### REFERENCES

- Bertiau, S. J. 1957, ApJ, 125, 696  
 Brown, T. M., & Gilliland, R. L. 1994, ARA&A, 32, 37  
 Brown, T. M., Noyes, R. W., Nisenson, P., Korzennik, S., & Horner, S. 1994, PASP, 106, 1285  
 Christensen-Dalsgaard, J., Bedding, T. R., & Kjeldsen, H. 1995, ApJ, 443, L29  
 Guenther, D. B., & Demarque, P. 1996, ApJ, 456, 798  
 Kjeldsen, H., Bedding, T. R., Viskum, M., & Frandsen, S. 1995, AJ, 109, 1313 (KBVF)  
 Régulo, C., Jiménez, A., Pallé, P. L., Pérez Hernández, F., & Roca Cortés, T. 1994, ApJ, 434, 384  
 Roberts, D. H., Lehar, J., & Dreher, J. W. 1987, AJ, 93, 968  
 Ronan, R. S., Harvey, J. W., & Duvall, T. L., Jr. 1991, ApJ, 369, 549  
 Scargle, J. D. 1982, ApJ, 263, 835